

This article was downloaded by:

On: 23 January 2011

Access details: *Access Details: Free Access*

Publisher *Taylor & Francis*

Informa Ltd Registered in England and Wales Registered Number: 1072954 Registered office: Mortimer House, 37-41 Mortimer Street, London W1T 3JH, UK



Journal of Coordination Chemistry

Publication details, including instructions for authors and subscription information:

<http://www.informaworld.com/smpp/title~content=t713455674>

X-ray structure analysis and DFT study of a chiral (salen)Mn^{III} complex toward understanding of inversion of enantioselection in epoxidation catalysts

Andreas Scheurer^a; Ralph Puchta^{ab}; Frank Hampel^b

^a Department Chemie und Pharmazie, Anorganische Chemie, Universität Erlangen-Nürnberg, Egerlandstraße 1, 91058 Erlangen, Germany ^b Department Chemie und Pharmazie, Computer Chemistry Center, Universität Erlangen-Nürnberg, Nägelsbachstraße 25, 91052 Erlangen, Germany

Online publication date: 16 August 2010

To cite this Article Scheurer, Andreas , Puchta, Ralph and Hampel, Frank(2010) 'X-ray structure analysis and DFT study of a chiral (salen)Mn^{III} complex toward understanding of inversion of enantioselection in epoxidation catalysts', Journal of Coordination Chemistry, 63: 14, 2868 – 2878

To link to this Article: DOI: 10.1080/00958972.2010.508520

URL: <http://dx.doi.org/10.1080/00958972.2010.508520>

PLEASE SCROLL DOWN FOR ARTICLE

Full terms and conditions of use: <http://www.informaworld.com/terms-and-conditions-of-access.pdf>

This article may be used for research, teaching and private study purposes. Any substantial or systematic reproduction, re-distribution, re-selling, loan or sub-licensing, systematic supply or distribution in any form to anyone is expressly forbidden.

The publisher does not give any warranty express or implied or make any representation that the contents will be complete or accurate or up to date. The accuracy of any instructions, formulae and drug doses should be independently verified with primary sources. The publisher shall not be liable for any loss, actions, claims, proceedings, demand or costs or damages whatsoever or howsoever caused arising directly or indirectly in connection with or arising out of the use of this material.

X-ray structure analysis and DFT study of a chiral (salen)Mn^{III} complex toward understanding of inversion of enantioselection in epoxidation catalysts¶

ANDREAS SCHEURER*†, RALPH PUCHTA†‡ and FRANK HAMPEL§

†Department Chemie und Pharmazie, Anorganische Chemie, Universität Erlangen-Nürnberg, Egerlandstraße 1, 91058 Erlangen, Germany

‡Department Chemie und Pharmazie, Computer Chemistry Center, Universität Erlangen-Nürnberg, Nägelsbachstraße 25, 91052 Erlangen, Germany

§Department Chemie und Pharmazie, Organische Chemie, Universität Erlangen-Nürnberg, Henkestraße 1, 91054 Erlangen, Germany

(Received 1 June 2010; in final form 2 July 2010)

A new (salen)Mn^{III} chloro complex (**7**) has been prepared and characterized by elemental analysis, IR spectroscopy, FAB mass spectrometry, and X-ray crystallography. Single crystal X-ray structure analysis revealed that **7** crystallizes in the orthorhombic space group $P2_12_12$ with $a = 17.1585(4)$, $b = 18.2591(6)$, $c = 13.0476(3)$ Å, $V = 4087.80(19)$ Å³, and eight molecules in the unit cell. In contrast to the literature catalysts **1** and **2**, the heteroalkyl substituents near to the chiral centers in the diimine moiety of **7** are axial, leading to the inversion of enantioselection of former epoxidation catalysts **3**. In addition, the application of different DFT methods (UB3LYP/LANL2DZp, UBP86/LACVP*) showed that a possible Mn...OMe interaction, found in the solid state for **7A**, of the axial CH₂OMe substituent in the ligand backbone is very weak and, therefore, the inverted enantioselectivity compared to literature catalysts originates from the axial heteroalkyl backbone substituents.

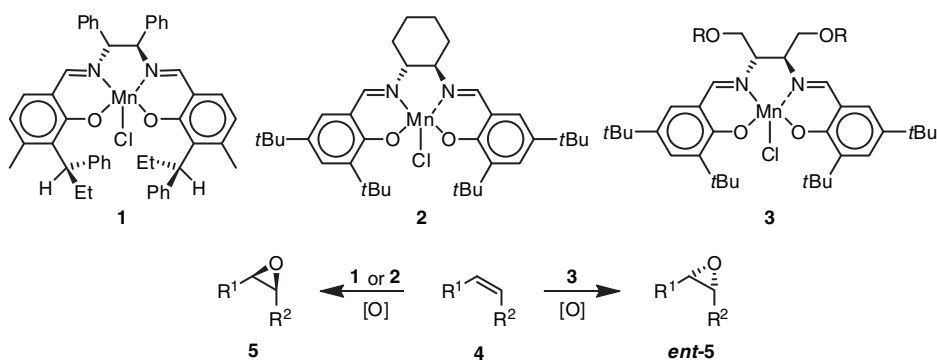
Keywords: (Salen)manganese(III) complex; N,O ligand; Conformation analysis; X-ray diffraction; Density functional calculations

1. Introduction

The need for efficient transformations of simple compounds into more useful, functionalized organic products has driven research toward a variety of catalytic concepts, for example, pure organo- [1] and metal-mediated asymmetric catalysis [2] in homo- [3] or heterogeneous phases [4] and with different solvent concepts [5]. For metal-mediated catalysis, a frequently employed and important metal is manganese for man-made [6] or *in-vivo* catalytic systems [7]. In addition to our research on manganese-based supramolecular assemblies for the construction of single-molecule magnets [8], we prepared and investigated, in the course of our catalysis studies [9], a series of

*Corresponding author. Email: andreas.scheurer@chemie.uni-erlangen.de

¶Dedicated to Prof. Rudi van Eldik on the occasion of his 65th birthday.



Scheme 1. Influence of the catalysts **1** or **2** vs. **3** on the stereochemistry of the asymmetric epoxidation of unfunctionalized olefins **4** to yield epoxides **5** and *ent-5*.

(salen)Mn^{III} complexes **3** (R = H, Me, Bn, -CH₂-2-naphthalene, trityl) [9a,b] analogous to well-known catalysts **1** and **2** studied by Katsuki [10] and Jacobsen [11] for asymmetric epoxidation of unfunctionalized olefins [12] (scheme 1), which still remains an active field of research [13]. Compared to the obtained stereochemistry of epoxides **5** reported with catalysts **1** and **2**, stereochemically identical **3** afforded *ent-5* with opposite configuration (*ee* up to 69%) from (*Z*)-alkenes **4** such as chromenes, 1,2-dihydronaphthalene, and indene.

The origin of the inverse enantioselection caused by the L-tartaric acid-derived [14] catalysts **3** is likely based on the possible axial position [15] of the acyclic heteroalkyl substituents [16] in the diimine backbone. This surprising observation was reinvestigated and confirmed by an independent study on the asymmetric epoxidation of indene, catalyzed by **3** (R = H, Bn) [16g]. However, the arguments for the inversion of enantioselectivity remain rather speculative. Therefore, we studied diamagnetic (salen)Ni^{II} complexes, analogous to **3**, as catalytic active model systems [9d] by quantum-chemical calculations, ¹H NMR spectroscopy, and single-crystal X-ray structure analysis. As expected the (salen)Ni^{II} complexes revealed axial conformation of the acyclic heteroalkyl substituents in the diimine backbone and an almost perfect square-planar environment at the nickel centers.

2. Experimental

2.1. General techniques

Unless stated otherwise, all manipulations were carried out under dry dinitrogen and the solvents used were purified and dried according to standard procedures. All reagents employed (high-grade purity materials) were commercially available and used as supplied (Fluka, Aldrich, and Acros Organics). Melting points were determined on a WAGNER-MUNZ apparatus and are not corrected. IR spectra were recorded from CHBr₃ triturations (NaCl pellets) with a Bruker IFS 25 spectrometer. FAB-MS spectra were recorded on a Jeol JMS-700 spectrometer with xenon as the bombarding gas and

m-NBA as matrix. Elemental analyses were performed on a Carlo Erba EA1110 CHN instrument and on a HERAEUS CHN-Mikroautomat.

2.2. Synthesis of (2*S*,3*S*)-1,4-dimethoxy-2,3-bis[(salicylidene)amino]butane (6)

For the experimental data of 6, see ref. [9d].

2.3. (2*S*,3*S*)-[*N,N*-Bis(salicylidene)-1,4-dimethoxy-2,3-diaminobutane] manganese(III) chloride (7)

A two-neck round-bottom flask equipped with a reflux condenser and a septum was charged with salen (0.178 mg, 0.5 mmol) and EtOH (27.5 mL). After heating to reflux, a solution of Mn(OAc)₂·4H₂O (245 mg, 1.0 mmol) in distilled water (2.5 mL) was added *via* syringe. The resulting brown solution was further refluxed for 60 min. Then still at boiling, air was bubbled into the solution for 15 min. Brine (1.5 mL) was added and the brown reaction mixture was refluxed for additional 30 min. After cooling to room temperature and standing without stirring overnight, the formed brown solid was filtered and washed with cold MeOH. Drying under vacuum and recrystallization from chloroform by vapor diffusion of *n*-pentane afforded the (salen)Mn^{III} chloro complex 7 as deep brown crystals, suitable for X-ray analysis. Yield: 180 mg (81%); m.p. >270°C (decomp.); IR: $\bar{\nu}$ =2960, 2905, 2868, 1616, 1598, 1553, 1532, 1475, 1460, 1428, 1412, 1390, 1361, 1307, 1270, 1252, 1199, 1032, 971, 875, 840, 812, 781, 759 cm⁻¹; MS: *m/z* (%)=444 (11) [M]⁺, 409 (100) [M–Cl]⁺; elemental analysis Calcd for C₂₀H₂₂ClMnN₂O₄ (444.79) (%): C, 54.01; H, 4.99; N, 6.30; Found (%): C, 53.98; H, 5.03; N, 6.34.

2.4. Single crystal X-ray structure analyses

Details of crystal data, data collection, and refinement are given in table 1. X-ray data for 7 were collected on a Nonius KappaCCD area detector, with Mo-K α radiation (λ =0.71073 Å). The structures were solved by direct methods with SHELXS-97 and refined with full-matrix least-squares against F^2 with the SHELXL-97 program system [17]. Lorentz, polarization, and absorption corrections were applied [18]. All non-hydrogen atoms were refined anisotropically. The positions of the hydrogens were fixed in ideal positions (riding model) and were included without refinement and with fixed isotropic *U*. The independent molecule 7A showed disorder on one OCH₃ moiety (O4/O4a and C6/C6a) with a refined occupation of the two preferred orientations of 49% and 51%.

2.5. Computational details

All structures were fully optimized using the B3LYP hybrid density functional [20] and the LANL2DZ basis set augmented with polarization functions (further denoted as LANL2DZp) [21–24]. All structures were characterized as minima by the computation of vibrational frequencies and the stability of the wave function was tested. The influence of bulk solvent was probed by single-point calculations employing the CPCM

Table 1. Crystal data, data collection, and structure refinement details for X-ray structure determination of **7**.

Empirical formula	C ₂₀ H ₂₂ ClMnN ₂ O ₄
Formula weight (g mol ⁻¹)	444.79
Temperature (K)	173(2)
Crystal size (mm ³)	0.20 × 0.20 × 0.10
Crystal system	Orthorhombic
Space group	<i>P</i> 2 ₁ 2 ₁ 2
Unit cell dimensions (Å, °)	
<i>a</i>	17.1585(4)
<i>b</i>	18.2591(6)
<i>c</i>	13.0476(3)
Volume (Å ³), <i>Z</i>	4087.8(2), 8
ρ_{Calcd} (Mg m ⁻³)	1.445
Absorption coefficient (mm ⁻¹)	0.805
<i>F</i> (000)	1840
θ range (°)	2.26–25.04
Index ranges	–20 ≤ <i>h</i> ≤ 20; –21 ≤ <i>k</i> ≤ 21; –15 ≤ <i>l</i> ≤ 15
Reflections collected	7200
Independent reflections	7200
Reflections observed [<i>I</i> > 2σ(<i>I</i>)]	6452
Max. and min. transmission	0.9239/0.8557
Data/restraints/parameters	7200/2/512
Goodness-of-fit on <i>F</i> ²	1.080
Flack parameter ^a	0.00(2)
Final <i>R</i> ₁ [<i>I</i> > 2σ(<i>I</i>)]	0.0486
<i>wR</i> ₂ (all data)	0.1331
Largest residuals (e Å ⁻³)	0.813/–0.398

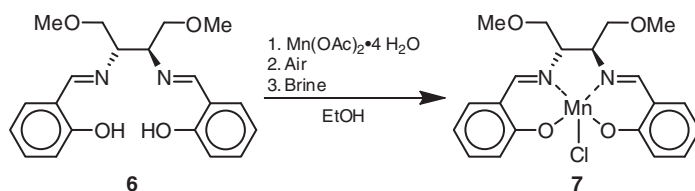
^aReference [19].

formalism [25] with water as solvent, i.e., B3LYP(CPCM:H₂O)/LANL2DZp//B3LYP/LANL2DZp. The Gaussian 03 suite of programs was used [26]. Additional structure optimizations were carried out with Jaguar 6.5 [27] applying the pure density functional BP86 [28] together with the LACVP* basis set [22,29] for structure calculations in the gas phase [30] and optimization including the water model [BP86(H₂O)/LACVP*] [31] as implemented in Jaguar 6.5. All energy values were evaluated by MP2(fc) calculations [32].

3. Results and discussion

3.1. Synthesis

Compared to our (salen)Ni^{II} model systems, the Mn^{III} in salen complexes prefer higher coordination numbers than four and exhibit in case of a distorted octahedral coordination environment a Jahn–Teller (JT) axial elongation [33]. Being aware that these facts could have influence on the position (axial vs. equatorial) of the acyclic heteroalkyl substituents in the diimine, we decided to further investigate our (salen)Mn^{III} chloro system **3**. Since it was not possible to grow single crystals of **3**, we chose the simple (salen)Mn^{III} chloro complex **7** as the model complex. For that



Scheme 2. Synthesis of (salen) Mn^{III} chloro complex **7** from C_2 -symmetric salen ligand **6**.

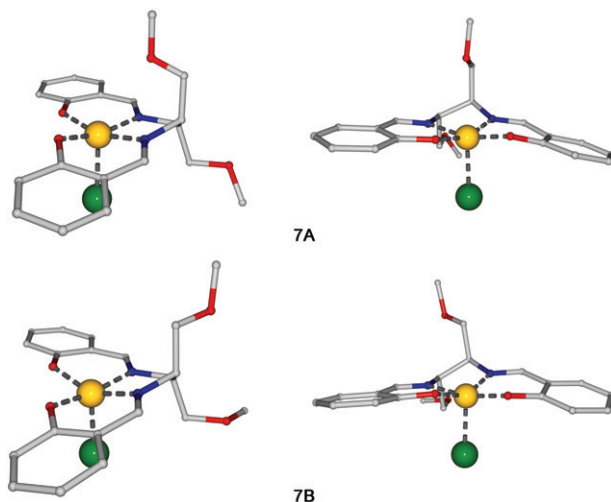


Figure 1. Molecular structures of the independent molecules **7A** (top) and **7B** (bottom) highlighting the axial positions and different orientation of the CH_2OMe groups as well as the slightly distorted square pyramidal coordination spheres at Mn^{III} . Left: view along the HC-CH bond of the diimine moiety; for **7A** a weak intramolecular $\text{Mn}^{\text{III}} \cdots \text{OMe}$ contact ($d_{\text{Mn}^{\text{III}} \cdots \text{OMe}} = 3.24 \text{ \AA}$) is observed. Right: front view from the $\text{O}_2\text{N}_2\text{Cl}$ coordinated Mn^{III} centers toward the chiral centers in the ligand backbone [POVRAY presentations; hydrogens and disorder omitted for clarity; Mn^{III} gold, Cl green, O red, N blue, C gray (color online)].

purpose, salen ligand **6**, generated from a C_2 -symmetric L-tartaric acid-derived vicinal diamine [14e], was treated with manganese(II) acetate tetrahydrate (scheme 2). The formed Mn^{II} intermediate was oxidized by bubbling air through the ethanolic solution and after anion exchange by the addition of brine the (salen) Mn^{III} chloro complex **7** could be isolated as a brown microcrystalline solid [9a].

3.2. Single-crystal X-ray structure analysis

Suitable crystals for an X-ray structural analysis were obtained from chloroform solutions of **7** by vapor diffusion of *n*-pentane. The (salen) Mn^{III} chloro complex **7** crystallizes in the orthorhombic space group $P2_12_12$ [34, 35], and the unit cell consists of two independent molecules **7A** and **7B** which exhibit small differences in bond lengths and angles as well as disorder of an OMe group (figure 1, table 2). In the solid state a slightly distorted square pyramidal coordination environment ($\text{O}_2/\text{N}_2/\text{Cl}$ ligation) was found for the manganese in **7** (figure 1). Furthermore, both CH_2OMe substituents in the

Table 2. Key structural data for two independent molecules **7A** and **7B** found in the unit cell.

Bond lengths (Å) and angles (°) ^a	Independent molecule 7A with Mn ^{III} ...OMe contact ^b	Independent molecule 7B without Mn ^{III} ...OMe contact ^c
Mn(1)–O(2)	1.868(3)	1.855(3)
Mn(1)–O(1)	1.883(3)	1.889(3)
Mn(1)–N(2)	1.975(3)	1.983(4)
Mn(1)–N(1)	1.986(4)	1.967(3)
Mn(1)–O(4)	3.2430 ^d	4.7722(1)
Mn(1)–O(3)	4.8349(1)	4.8219(1)
Mn(1)–Cl(1)	2.3872(14)	2.3554(16)
∠O(2)–Mn(1)–O(1)	91.59(15)	90.56(14)
∠N(2)–Mn(1)–N(1)	81.62(15)	81.43(15)
∠H(2)–C(2)–C(3)–H(3)	–82.67	–81.87
∠N(1)–C(2)–C(3)–N(2)	41.61	40.21

^aThe identical numbering of the heavy atoms in the X-ray data of the two independent molecules **7A** and **7B** is differentiated by an addition of prime symbol (') and is omitted in this listing.

^bFigure 1 top.

^cFigure 1 bottom.

^dMn(1)–O(4A), the other disordered OMe group showed a distance $d_{\text{Mn(1)-O(4)}} = 4.1966(1) \text{ \AA}$.

diimine ligand backbone are axial, causing the inversed enantioselection of complexes **3** [36] compared to **1** and **2**. For the independent molecules **7A** present in the unit cell a weak *intramolecular* Mn^{III}...OMe coordination of one ether arm was identified ($d_{\text{Mn}\dots\text{OMe}} = 3.24 \text{ \AA}$), which is even shorter than those in the Ni^{II}...OMe case [9d, 14a] (*intermolecular* $d_{\text{Ni}\dots\text{OMe}} = 3.55 \text{ \AA}$, leading to the formation of enantiomerically pure helical 1-D coordination polymers in the solid state and on highly oriented pyrolytic graphite). Despite the presence of phenyl rings in the salen ligand of **7**, no π – π interaction could be detected in the packing of the molecules in the crystal.

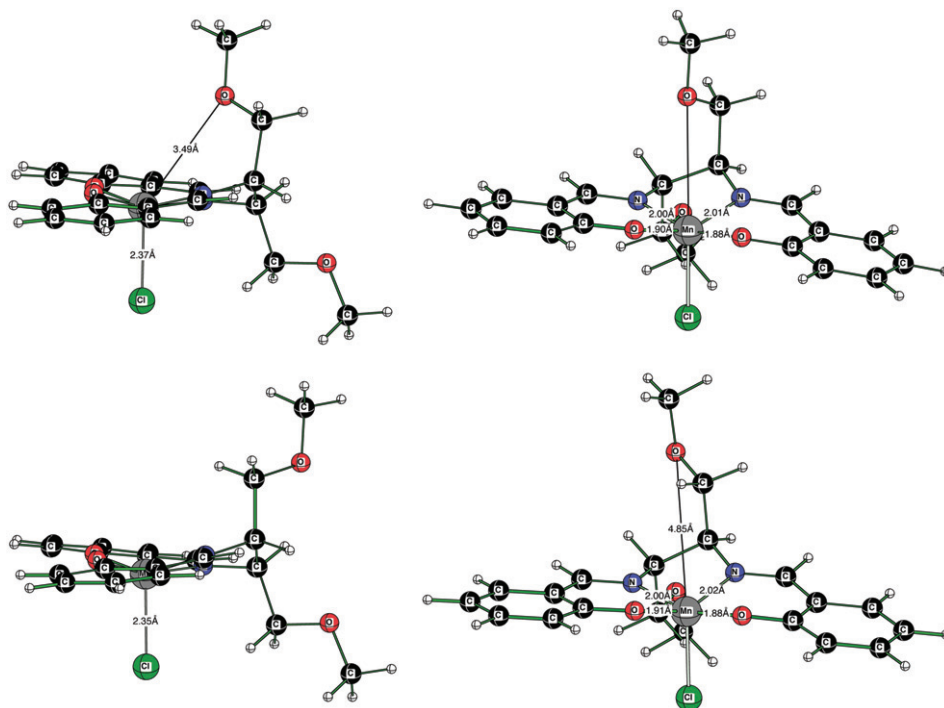
3.3. Quantum-chemical calculations

Motivated by the crystallographically observed weak intramolecular Mn^{III}...OMe contact, we became interested if the ether oxygen can strongly interact with the manganese and therewith influence the catalytic epoxidation reaction. An appropriate tool, widely used for the investigation of (salen) transition metal complexes is the application of quantum chemistry, especially density functional theory [36, 37]. Comparisons of the computed structures show, within the accuracy of the calculations, that independent from the method and even if solvent effects have been included or not, the structural data of the (salen)Mn^{III} moiety are nearly identical (table 3, figures 2 and 3).

Neither the Mn...OMe distances in the gas phase calculations of 3.40 Å (UBP86/LACVP*) and 3.49 Å (UB3LYP/LANL2DZp) nor the significantly shorter distance of the calculation including a solvent model ($d_{\text{Mn}\dots\text{OMe}} = 3.17 \text{ \AA}$) (UBP86(H₂O)/LACVP*) suggests a strong Mn...OMe interaction for the rotamer (figures 2 and 3, respectively), where the oxygen is oriented toward the Mn^{III}. While the calculation within the solvent model shortens the distance between the manganese and the ether oxygen compared to the gas phase calculation, it elongates the Mn–Cl distance. In the rotamer with the ether moiety facing away from the manganese center the Mn...OMe distance is shortened by 0.06 to 4.78 Å (UBP86/LACVP* vs. UBP86(H₂O)/LACVP*),

Table 3. Key structure features of the calculated rotamers considering different quantum-chemical approaches.

Bond lengths (Å) and angles (°)	UB3LYP/ LANL2DZp with contact	UB3LYP/ LANL2DZp without contact	UBP86/ LACVP* with contact	UBP86/ LACVP* without contact	UBP86(H ₂ O)/ LACVP* with contact	UBP86(H ₂ O)/ LACVP* without contact
Mn–O	1.88/1.90	1.88/1.91	1.88/1.89	1.87/1.89	1.88/1.88	1.88/1.88
M–N	2.02/2.00	2.03/2.00	2.00/1.99	2.00/2.00	1.98/1.98	1.98/1.99
Mn···OMe	3.49	4.85	3.40	4.84	3.17	4.78
Mn–Cl	2.37	2.35	2.39	2.38	2.49	2.48
∠O–Mn–O	92.0	92.1	91.5	91.2	92.6	92.7
∠N–Mn–N	81.1	80.6	81.5	81.0	82.5	81.9
Φ H–CR–CR–H	–83.9	–79.2	–83.8	–81.2	–80.9	–80.2
Φ N–CR–CR–N	37.4	41.1	37.8	39.7	40.1	40.8

Figure 2. Calculated (UB3LYP/LANL2DZp) structures without consideration of solvent effects [MOLECULE presentations; Mn^{III} gray, Cl green, O red, N blue, C black, and H white (color online)].

too, but not so pronounced as in the rotamer with the weak Mn···OMe contact. Comparing the structural data from the solid state with the quantum-chemical calculations no huge differences can be observed, but the UBP86(H₂O)/LACVP*-calculations fit best in this case (tables 2 and 3).

The finding of a very weak OMe ether contact to the Mn^{III} center is further supported by the energy gap of the rotamers (table 4). Note that the observed energy gaps are close to the limit of the applied quantum-chemical methods.

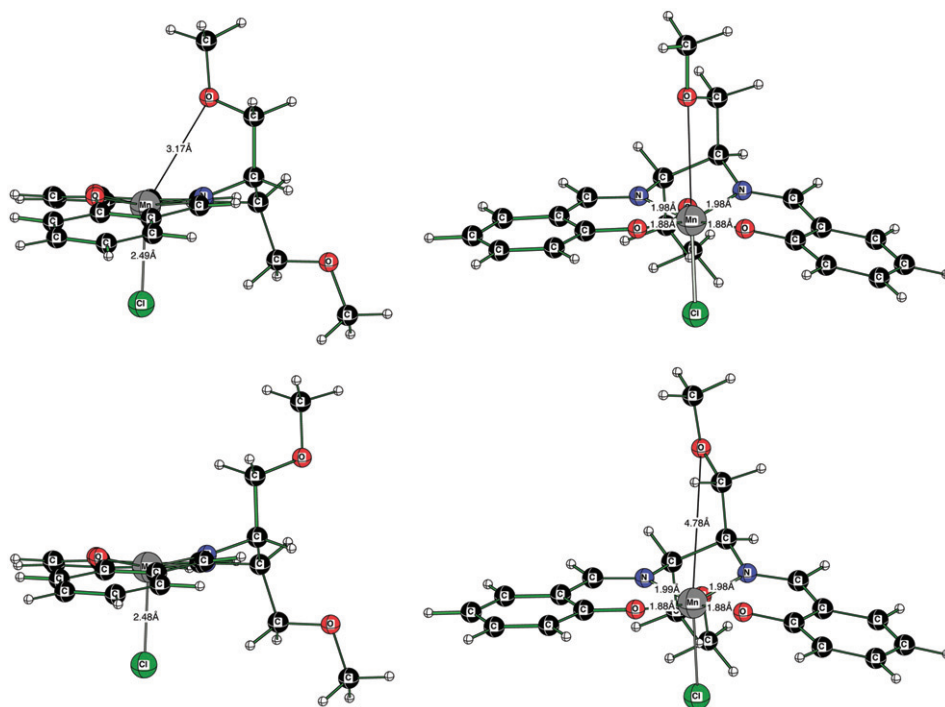


Figure 3. Calculated (UBP86(H₂O))/LACVP* structures with consideration of solvent effects [molecule presentations; Mn^{III} gray, Cl green, O red, N blue, C black, and H white (color online)].

Table 4. Calculated relative stabilities of the rotamers considering different quantum-chemical approaches.

Quantum-chemical approach	With contact (kcal mol ⁻¹)	Without contact (kcal mol ⁻¹)
UB3LYP/LANL2DZp//UB3LYP/LANL2DZp + ZPE(UB3LYP/LANL2DZp)	0.0	-1.0
UMP2(fc)/LANL2DZp//UB3LYP/LANL2DZp + ZPE(UB3LYP/LANL2DZp)	0.0	+0.2
UB3LYP(CPCM:H ₂ O)/LANL2DZp//UB3LYP/ LANL2DZp + ZPE(UB3LYP/LANL2DZp)	0.0	-0.2
UBP86/LACVP*//UBP86/LACVP* + ZPE(UB3LYP/LANL2DZp)	0.0	-0.6
UMP2(fc)/LACVP*//UBP86/LACVP* + ZPE(UB3LYP/LANL2DZp)	0.0	+1.0
UBP86(H ₂ O)/LACVP*//UBP86(H ₂ O)/LACVP* + ZPE(UB3LYP/LANL2DZp)	0.0	+0.3
UMP2(fc)/LACVP*//UBP86(H ₂ O)/LACVP* + ZPE(UB3LYP/LANL2DZp)	0.0	+2.3

Independent from the selected quantum-chemical method, there is no clear and significant preference for one of the investigated rotamers. Energetically both rotamers seem to be essentially equal. As neither strong Mn...OMe coordination nor some steric hindrances are included in the molecule, one can expect basically free rotation of the ether moiety.

The interaction of the ether oxygen to the Mn^{III} center seems to be too weak to influence the catalysis pathway. Despite the fact that these findings are based on the catalyst precursor and not on the catalytic active species or even the transition state

[12b, 38], we attribute the inversion of the enantioselection to the axial conformation of the acyclic heteroalkyl substituents in the ligand backbone of **3** and **7** as suggested previously [9d,36].

4. Conclusion

The (salen)Mn^{III} chloro complex **7**, a model for our previously investigated catalysts **3**, was studied by single-crystal X-ray structure analysis and quantum-chemical calculations. All investigations established an axial position of the CH₂-OMe ether substituent in the diimine. The origin for the reversed enantioselection caused by **3** (compared to Katsuki's or Jacobsen's catalysts **1** and **2**) is basically due to the axial positions of the acyclic heteroalkyl substituent in the ligand backbone, as possible Mn...OMe interactions, deduced from quantum-chemical calculations, turned out to be very weak.

Acknowledgments

The authors would like to thank Prof. Dr R.W. Saalfrank for his endorsement to perform this research. This work was supported by the Deutsche Forschungsgemeinschaft SPP 1137 *Molecular Magnetism* (SA 276/26-1-3), SA 276/27-1-2 and SA 276/29-1. We would like to thank Prof. T. Clark for hosting this work in the CCC and the Regionales Rechenzentrum Erlangen (RRZE) for a generous allotment of computer time. Finally, the generous allocation of premises by Prof. Dr K. Meyer at the Lehrstuhl für Anorganische und Allgemeine Chemie (Universität Erlangen-Nürnberg) is gratefully acknowledged.

References

- [1] A. Berkessel, H. Gröger. *Asymmetric Organocatalysis*, 1st Edn, Wiley-VCH, Weinheim (2005).
- [2] K. Mikami, M. Lautens (Eds). *New Frontiers in Asymmetric Catalysis*, 1st Edn, John Wiley & Sons, Inc., Hoboken, New Jersey (2007).
- [3] B. Cornils, W.A. Herrmann, I.T. Horvath, W. Leitner, S. Mecking, H. Olivier-Bourbigou, D. Vogt (Eds). *Multiphase Homogeneous Catalysis*, 1st Edn, Wiley-VCH, Weinheim (2005).
- [4] G. Ertl, H. Knözinger, F. Schüth, J. Weitkamp (Eds). *Handbook of Heterogeneous Catalysis*, 2nd Edn, Wiley-VCH, Weinheim (2008).
- [5] (a) P.G. Jessop, W. Leitner (Eds). *Chemical Synthesis Using Supercritical Fluids*, 1st Edn, Wiley-VCH, Weinheim (1999); (b) P. Wasserscheid, T. Welton (Eds). *Ionic Liquids in Synthesis*, 2nd Edn, Wiley-VCH, Weinheim (2007); (c) D.J. Adams, P.J. Dyson, S.J. Tavener, *Chemistry in Alternative Reaction Media*, 1st Edn, John Wiley & Sons Ltd., Chichester, West Sussex (2004).
- [6] (a) B. Meunier. *Chem. Rev.*, **92**, 1411 (1992); (b) E. Ember, H.A. Gazzaz, S. Rothbart, R. Puchta, R. van Eldik. *Appl. Catal. B: Environmental*, **95**, 179 (2010); (c) G.-F. Liu, K. Dürr, R. Puchta, F.W. Heinemann, R. van Eldik, I. Ivanović-Burmazović. *Dalton Trans.*, 6292 (2009); (d) A. Dees, A. Zahl, R. Puchta, N.J.R. van Eikema Hommes, F.W. Heinemann, I. Ivanović-Burmazović. *Inorg. Chem.*, **46**, 2459 (2007).
- [7] (a) D.W. Christianson, J.D. Cox. *Annu. Rev. Biochem.*, **68**, 33 (1999); (b) J. Dasgupta, G.M. Ananyev, G.C. Dismukes. *Coord. Chem. Rev.*, **252**, 347 (2008).

- [8] (a) N. Schmidt, A. Scheurer, S. Sperner, R.H. Fink. *Z. Naturforsch. B*, **65**, 390 (2010); (b) R.W. Saalfrank, H. Maid, A. Scheurer. *Angew. Chem.*, **120**, 8924 (2008); *Angew. Chem. Int. Ed.*, **47**, 8794 (2008); (c) R.W. Saalfrank, A. Scheurer, R. Prakash, F.W. Heinemann, T. Nakajima, F. Hampel, R. Leppin, B. Pilawa, H. Rupp, P. Müller. *Inorg. Chem.*, **46**, 1586 (2007); (d) R.W. Saalfrank, T. Nakajima, N. Mooren, A. Scheurer, H. Maid, F. Hampel, C. Trieflinger, J. Daub. *Eur. J. Inorg. Chem.*, 1149 (2005).
- [9] (a) A. Scheurer, P. Mosset, M. Spiegel, R.W. Saalfrank. *Tetrahedron*, **55**, 1063 (1999); (b) A. Scheurer, P. Mosset, M. Spiegel, R.W. Saalfrank. In *Peroxide Chemistry, Mechanistic and Preparative Aspects of Oxygen Transfer*, W. Adam (Ed.), pp. 320–340, Wiley-VCH, Weinheim (2000); (c) R. Boulch, A. Scheurer, P. Mosset, R.W. Saalfrank. *Tetrahedron Lett.*, **41**, 1023 (2000); (d) A. Scheurer, H. Maid, F. Hampel, R.W. Saalfrank, L. Toupet, P. Mosset, R. Puchta, N.J.R. van Eikema Hommes. *Eur. J. Org. Chem.*, 2566 (2005).
- [10] R. Irie, K. Noda, Y. Ito, N. Matsumoto, T. Katsuki. *Tetrahedron Lett.*, **31**, 7345 (1990).
- [11] W. Zhang, J.L. Loebach, S.R. Wilson, E.N. Jacobsen. *J. Am. Chem. Soc.*, **112**, 2801 (1990).
- [12] (a) E.M. McGarrigle, D.G. Gilheany. *Chem. Rev.*, **105**, 1563 (2005); (b) T. Katsuki. *Adv. Synth. Catal.*, **344**, 131 (2002); (c) E.N. Jacobsen, M.H. Wu. In *Comprehensive Asymmetric Catalysis*, E.N. Jacobsen, A. Pfaltz, H. Yamamoto (Eds), pp. 649–679, Springer-Verlag, Berlin (1999).
- [13] (a) M.E. Amato, F.P. Ballistreri, A. Pappalardo, G.A. Tomaselli, R.M. Toscano. *Molecules*, **15**, 1442 (2010); (b) S. Liao, B. List. *Angew. Chem.*, **122**, 638 (2010); *Angew. Chem. Int. Ed.*, **49**, 628 (2010); (c) K. Matsumoto, T. Oguma, T. Katsuki. *Angew. Chem.*, **121**, 7568 (2009); *Angew. Chem. Int. Ed.*, **48**, 7432 (2009); (d) A.D. Garnovskii, I.S. Vasilchenko, D.A. Garnovskii, B.I. Kharisov. *J. Coord. Chem.*, **62**, 151 (2009); (e) K. Matsumoto, T. Kubo, T. Katsuki. *Chem. Eur. J.*, **15**, 6573 (2009); (f) K.C. Gupta, A.K. Sutar. *Coord. Chem. Rev.*, **252**, 1420 (2008); (g) S.T. Oyama. In *Mechanisms in Homogeneous and Heterogeneous Epoxidation Catalysis*, S.T. Oyama (Ed.), pp. 3–99, Elsevier, Amsterdam (2008); (h) D. Chatterjee, S. Basak, J. Muzart. *J. Mol. Catal. A: Chem.*, **271**, 270 (2007); (i) S. Zhao, J. Zhao, D. Zhao. *Carbohydr. Res.*, **342**, 254 (2007); (j) F.P. Ballistreri, A. Patti, S. Pedotti, G.A. Tomaselli, R.M. Toscano. *Tetrahedron: Asymmetry*, **18**, 2377 (2007); (k) O.A. Wong, Y. Shi. *J. Org. Chem.*, **71**, 3973 (2006); (l) B. Akagah, F. Estour, P. Vérité, E. Seguin, F. Tillequin, O. Lafont. *J. Heterocycl. Chem.*, **42**, 1267 (2005).
- [14] For further work of our group on L-tartaric acid derived compounds, cf: (a) M.S. Alam, A. Scheurer, R.W. Saalfrank, P. Müller. *Z. Naturforsch.*, **63b**, 1443 (2008); (b) R.W. Saalfrank, C. Spitzlei, A. Scheurer, H. Maid, F.W. Heinemann, F. Hampel. *Chem. Eur. J.*, **14**, 1472 (2008); (c) R.W. Saalfrank, C. Schmidt, H. Maid, F. Hampel, W. Bauer, A. Scheurer. *Angew. Chem.*, **118**, 322 (2006); *Angew. Chem. Int. Ed.*, **45**, 315 (2006); (d) A. Scheurer, W. Bauer, F. Hampel, C. Schmidt, R.W. Saalfrank, P. Mosset, R. Puchta, N.J.R. van Eikema Hommes. *Tetrahedron: Asymmetry*, **15**, 867 (2004); (e) A. Scheurer, P. Mosset, R.W. Saalfrank. *Tetrahedron: Asymmetry*, **10**, 3559 (1999); (f) A. Scheurer, P. Mosset, R.W. Saalfrank. *Tetrahedron: Asymmetry*, **8**, 1243 and 3161 (1997).
- [15] (a) H. Shitama, T. Katsuki. *Chem. Eur. J.*, **13**, 4849 (2007); (b) Y.N. Ito, T. Katsuki. *Tetrahedron Lett.*, **39**, 4325 (1998).
- [16] For further work on salen complexes with oxygen functionalities in the ligand backbone, cf: (a) M. Schley, P. Lönnecke, E. Hey-Hawkins. *J. Organomet. Chem.*, **694**, 2480 (2009); (b) B. Saha, M.-H. Lin, T.V. RajanBabu. *J. Org. Chem.*, **72**, 8648 (2007); (c) C. Borriello, R. Del Litto, A. Panunzi, F. Ruffo. *Inorg. Chem. Commun.*, **8**, 717 (2005); (d) C. Borriello, R. Del Litto, A. Panunzi, F. Ruffo. *Tetrahedron: Asymmetry*, **15**, 681 (2004); (e) B.J. Paul, J. Willis, T.A. Martinot, I. Ghiviriga, K.A. Abboud, T. Hudlicky. *J. Am. Chem. Soc.*, **124**, 10416 (2002); (f) M.-H. Lin, T.V. RajanBabu. *Org. Lett.*, **4**, 1607 (2002); (g) A. Star, I. Goldberg, B. Fuchs. *J. Organomet. Chem.*, **630**, 67 (2001); (h) D. Bell, D. Miller, R.P. Attrill. *PCT Int. Appl. WO 94/03271* (1994); (i) D. Bell, F. Finney, R.P. Attrill, D. Miller. *PCT Int. Appl. WO 95/21172* (1995).
- [17] G.M. Sheldrick. *Acta Crystallogr., Sect. A*, **64**, 112 (2008).
- [18] (a) “Collect” data collection software. B.V. Nonius, Delft, The Netherlands (1998); (b) “Scalepack” data processing software. Z. Otwinowski, W. Minor, *Methods Enzymol.*, **276**, 307 (1997).
- [19] H.D. Flack. *Acta Crystallogr., Sect. A*, **39**, 876 (1983).
- [20] (a) A.D. Becke. *J. Chem. Phys.*, **98**, 5648 (1993); (b) C. Lee, W. Yang, R.G. Parr. *Phys. Rev. B*, **37**, 785 (1988); (c) P.J. Stephens, F.J. Devlin, C.F. Chabalowski, M.J. Frisch. *J. Phys. Chem.*, **98**, 11623 (1994).
- [21] T.H. Dunning Jr., P.J. Hay. In *Modern Theoretical Chemistry*, H.F. Schaefer III (Ed.), Vol. 3, pp. 1–28, Plenum, New York (1976).
- [22] (a) P.J. Hay, W.R. Wadt. *J. Chem. Phys.*, **82**, 270 (1985); (b) P.J. Hay, W.R. Wadt. *J. Chem. Phys.*, **82**, 284 (1985); (c) P.J. Hay, W.R. Wadt. *J. Chem. Phys.*, **82**, 299 (1985).
- [23] S. Huzinaga (Ed.). *Gaussian Basis Sets for Molecular Calculations*, Elsevier, Amsterdam (1984).
- [24] The performance of this computational level is well documented; see, e.g.: (a) R.W. Saalfrank, H. Maid, A. Scheurer, R. Puchta, W. Bauer. *Eur. J. Inorg. Chem.*, 2903 (2010); (b) R. Puchta, N. van Eikema Hommes, R. Meier, R. van Eldik. *Dalton Trans.*, 3392 (2006); (c) R. Puchta, A. Scheurer. *Z. Naturforsch.*, **65b**, 231 (2010); (d) R.W. Saalfrank, H. Maid, A. Scheurer, F.W. Heinemann,

- R. Puchta, W. Bauer, D. Stern, D. Stalke. *Angew. Chem.*, **120**, 9073 (2008); *Angew. Chem. Int. Ed.*, **47**, 8941 (2008); (e) R. Puchta, R. van Eldik. *Eur. J. Inorg. Chem.*, 1120 (2007).
- [25] J.B. Foresman, T.A. Keith, K.B. Wiberg, J. Snoonian, M.J. Frisch. *J. Phys. Chem.*, **100**, 16098 (1996). The default $e=78.39$ was used throughout.
- [26] M.J. Frisch, G.W. Trucks, H.B. Schlegel, G.E. Scuseria, M.A. Robb, J.R. Cheeseman, J.A. Montgomery Jr, T. Vreven, K.N. Kudin, J.C. Burant, J.M. Millam, S.S. Iyengar, J. Tomasi, V. Barone, B. Mennucci, M. Cossi, G. Scalmani, N. Rega, G.A. Petersson, H. Nakatsuji, M. Hada, M. Ehara, K. Toyota, R. Fukuda, J. Hasegawa, M. Ishida, T. Nakajima, Y. Honda, O. Kitao, H. Nakai, M. Klene, X. Li, J.E. Knox, H.P. Hratchian, J.B. Cross, V. Bakken, C. Adamo, J. Jaramillo, R. Gomperts, R.E. Stratmann, O. Yazyev, A.J. Austin, R. Cammi, C. Pomelli, J.W. Ochterski, P.Y. Ayala, K. Morokuma, G.A. Voth, P. Salvador, J.J. Dannenberg, V.G. Zakrzewski, S. Dapprich, A.D. Daniels, M.C. Strain, O. Farkas, D.K. Malick, A.D. Rabuck, K. Raghavachari, J.B. Foresman, J.V. Ortiz, Q. Cui, A.G. Baboul, S. Clifford, J. Cioslowski, B.B. Stefanov, G. Liu, A. Liashenko, P. Piskorz, I. Komaromi, R.L. Martin, D.J. Fox, T. Keith, M.A. Al-Laham, C.Y. Peng, A. Nanayakkara, M. Challacombe, P.M.W. Gill, B. Johnson, W. Chen, M.W. Wong, C. Gonzalez, J.A. Pople. *Gaussian 03*, Revision B.03, Gaussian Inc., Wallingford, CT (2004).
- [27] *Jaguar (Version 6.5)*, Schrödinger, LLC, New York, NY (2006).
- [28] (a) J.C. Slater, In *Quantum Theory of Molecules and Solids, Vol. 4: The Self-Consistent Field for Molecules and Solids*, McGraw-Hill, New York (1974); (b) J.P. Perdew, A. Zunger. *Phys. Rev. B: Condens. Matter Mater. Phys.*, **23**, 5048 (1981); (c) J.P. Perdew. *J. Phys. Rev. B: Condens. Matter Mater. Phys.*, **33**, 8822 (1986); *Phys. Rev. B: Condens. Matter Mater. Phys.* **34**, 7406 (1986) [Erratum]; (d) A.D. Becke. *Phys. Rev. A: Atom. Mol. Opt. Phys.*, **38**, 3098 (1988).
- [29] (a) R. Ditchfield, W.J. Hehre, J.A. Pople. *J. Chem. Phys.*, **54**, 724 (1971); (b) W.J. Hehre, R. Ditchfield, J.A. Pople. *J. Chem. Phys.*, **56**, 2257 (1972); (c) W.J. Hehre, J.A. Pople. *J. Chem. Phys.*, **56**, 4233 (1972); (d) P.C. Hariharan, J.A. Pople. *Theor. Chim. Acta*, **28**, 213 (1973); (e) J.S. Binkley, J.A. Pople. *J. Chem. Phys.*, **66**, 879 (1977); (f) M.M. Francl, W.J. Pietro, W.J. Hehre, J.S. Binkley, M.S. Gordon, D.J. DeFrees, J.A. Pople. *J. Chem. Phys.*, **77**, 3654 (1982).
- [30] The performance of this computational level is well documented; see, e.g.: (a) R. Müller, E. Hübner, N. Burzlaff. *Eur. J. Inorg. Chem.*, 2151 (2004); (b) L. Peters, E. Hübner, N. Burzlaff. *J. Organomet. Chem.*, **690**, 2009 (2005).
- [31] (a) D.J. Tannor, B. Marten, R. Murphy, R.A. Friesner, D. Sitkoff, A. Nicholls, M. Ringnald, W.A. Goddard III, B. Honig. *J. Am. Chem. Soc.*, **116**, 11875 (1994); (b) B. Marten, K. Kim, C. Cortis, R.A. Friesner, R.B. Murphy, M.N. Ringnald, D. Sitkoff, B. Honig. *J. Phys. Chem.*, **100**, 11775 (1996).
- [32] W.J. Hehre, L. Radom, P. von R. Schleyer, J.A. Pople. *Ab Initio. Molecular Orbital Theory*, Wiley, New York (1986).
- [33] E.g.: Y. Feng, C. Wang, Y. Zhao, J. Li, D. Liao, S. Yan, Q. Wang. *Inorg. Chim. Acta*, **362**, 3563 (2009).
- [34] For details of crystal data, data collection and refinement, *q. v.* table 1 and 2.4 *Single crystal X-ray structure analyses*.
- [35] CCDC 743717 (7) contains the supplementary crystallographic data for this article. These data can be obtained free of charge from the Cambridge Crystallographic data centre via www.ccdc.cam.ac.uk/data_request/cif (accessed July 30, 2010).
- [36] W. Chaladaj, J. Jurczak. *Chem. Commun.*, 6747 (2009).
- [37] E.g.: (a) A.E. Fagin, G. Wang, M.C. Lau, S. Gronert. *Org. Lett.*, **10**, 1771 (2008); (b) H. Jacobsen, L. Cavallo. *Organometallics*, **25**, 177 (2006); (c) D. Feichtinger, D.A. Plattner. *Chem. Eur. J.*, **7**, 591 (2001); (d) J. El-Bahraoui, O. Wiest, D. Feichtinger, D.A. Plattner. *Angew. Chem.*, **113**, 2131 (2001); *Angew. Chem. Int. Ed.*, **40**, 2073 (2001); (e) D.A. Plattner, D. Feichtinger, J. El-Bahraoui, O. Wiest. *Int. J. Mass Spectrom.*, **195/196**, 351 (2000); (f) L. Cavallo, H. Jacobsen. *Angew. Chem.*, **112**, 602 (2000); *Angew. Chem. Int. Ed.*, **39**, 589 (2000).
- [38] (a) P.J. Pospisil, D.H. Carsten, E.N. Jacobsen. *Chem. Eur. J.*, **2**, 974 (1996); (b) D. Feichtinger, D.A. Plattner. *Chem. Eur. J.*, **7**, 591 (2001); (c) T. Kurahashi, M. Hada, H. Fujii. *J. Am. Chem. Soc.*, **131**, 12394 (2009); (d) T. Kurahashi, H. Fujii. *Inorg. Chem.*, **47**, 7556 (2008).